Anomalous X-Ray Scattering Measurement of Near-Neighbor Individual Pair Displacements and Chemical Order in $Fe_{22.5}Ni_{77.5}$

G. E. Ice, C. J. Sparks, and A. Habenschuss
Oak Ridge National Laboratory, Oak Ridge, Tennessee 37831

L. B. Shaffer
Department of Physics, Anderson University, Anderson, Indiana 46012
(Received 15 November 1991)

We demonstrate an anomalous-x-ray-diffraction procedure for the determination of pair correlations in crystalline solid solutions. This procedure experimentally removes the large thermal diffuse scattering background with no assumptions and permits separation of chemically specific static displacements. We recover the near-neighbor chemical order and static displacements in a $Fe_{22.5}Ni_{77.5}$ single crystal quenched from 1000 °C. The Fe-Fe nearest-neighbor distance is dilated by -0.043 Å from the average lattice. The possible magnetic origins of this dilation are discussed.

PACS numbers: 75.50.−y, 35.20.Dp, 81.40.Cd

Knowledge of the local structure of crystalline solid solutions is fundamental to understanding their physical and chemical properties. Short-range-order (SRO) coefficients which describe local chemical order [1] are used to determine pair potentials [2], to predict phase stability [3], and to compare directly with theoretical predictions [4]. Interatomic distances give insight into electronic properties, chemical and magnetic forces, and solid solution strengthening which affect the properties of an alloy [5].

We apply synchrotron radiation to measure multiple-wavelength diffuse x-ray scattering to determine chemically specific pair displacements as previously suggested [6]. Alternative techniques [7,8] are much less sensitive to the chemically specific displacements. We briefly review the theory of x-ray scattering from a cubic binary alloy single crystal with SRO and with both dynamic and static displacements to show how the local arrangements of atoms are obtained in a direct way.

The total elastic x-ray intensity I_T, in electron units, scattered by a crystal of N atoms with C_A and C_B the number fractions of A and B atoms having complex scattering factors f_A and f_B, long-range crystalline periodicity $\mathbf{R}_t$, and thermal and static displacement $\boldsymbol{\delta}_t$ from sites of the average lattice is given in kinematic theory by

$$I_T = I(h)_{\text{fund}} + I(h)_{\text{SRO}} + I(h)_{\text{SD}} = \sum_t \sum_q (C_A f_A + C_B f_B)^2 e^{i\mathbf{k}\cdot(\mathbf{R}_t - \mathbf{R}_q)} \langle e^{i\mathbf{k}\cdot(\boldsymbol{\delta}_t - \boldsymbol{\delta}_q)} \rangle \tag{1a}$$

$$+ N C_A C_B (f_A - f_B)^2 \sum_l \sum_m \sum_n \alpha_{lmn} e^{-2M\phi_{lmn}} \cos(2\pi h_1 l) \cos(2\pi h_2 m) \cos(2\pi h_3 n) \tag{1b}$$

$$+ 2N C_A C_B \operatorname{Re}\left[(f_A^* - f_B^*) \left(f_A \sum_{p=1,3} h_p Q_p^{AA} - f_B \sum_{p=1,3} h_p Q_p^{BB} \right) \right], \tag{1c}$$

where

$$Q_p^{AA} = -\pi \sum_l \sum_m \sum_n (C_A/C_B + \alpha_{lmn}) \langle \Delta_p \rangle_{lmn}^{AA} \sin(2\pi h_p l) \cos(2\pi h_{p+1} m) \cos(2\pi h_{p+2} n), \tag{1d}$$

and similarly for Q_p^{BB} [9]. The subscript p denotes one of the three directions of the lattice Cartesian coordinates, with subscripts $p+1$ and $p+2$ calculated modulo 3. The sum is over all t,q atom pairs with a time average of the thermal motion. Values of $\mathbf{k}\cdot\mathbf{R}$ and $\mathbf{k}\cdot\boldsymbol{\delta}$ are expressed in terms of the integer indices of the atom positions in the unit cell (l,m,n), continuously varying pure numbers in reciprocal space (h_1,h_2,h_3), and the three components of the atom displacements $(\Delta_1,\Delta_2,\Delta_3)$. The static displacement term $I(h)_{\text{SD}}$ is an approximation to first order (even orders are zero). Thermal motion is included to infinite order in the harmonic approximation. The term $e^{-2M\phi_{lmn}}$ accounts for the few-percent effect of thermal displacements on the SRO intensity distribution [10]. We seek to recover the static displacements $\langle\Delta\rangle$'s and the Warren-Cowley SRO parameters α's [1]. Both $I(h)_{\text{SRO}}$ and the aperiodic atomic displacement intensity $I(h)_{\text{SD}}$ depend on $f_{\text{Ni}} - f_{\text{Fe}}$, Eqs. (1b) and (1c) [9–11]. I_{fund}, Eq. (1a), is independent of order and can be measured by selecting an x-ray energy where $f_{\text{Ni}} - f_{\text{Fe}}$ approaches zero. At other x-ray energies $I(h)_{\text{SRO}}$ and $I(h)_{\text{SD}}$ are then obtained by subtracting scaled values of I_{fund} from the total diffuse intensity. Two linearly independent measurements of $I(h)_{\text{SD}}$ permit a separation of Q^{AA} and Q^{BB}. Q^{AB} is defined by Q^{AA} and Q^{BB} [9–11]. X-ray energies just below the absorption edges of Fe and Ni are selected to alter both the magnitude and the sign of $f_{\text{Ni}} - f_{\text{Fe}}$. Changes in the real, f', and imaginary, f'', terms of the complex x-ray scattering amplitude of an element, $f = f_0 + f' + if''$, can be a significant fraction of f_0 [12]. Alternative methods to separate out I_{fund} involve assump-

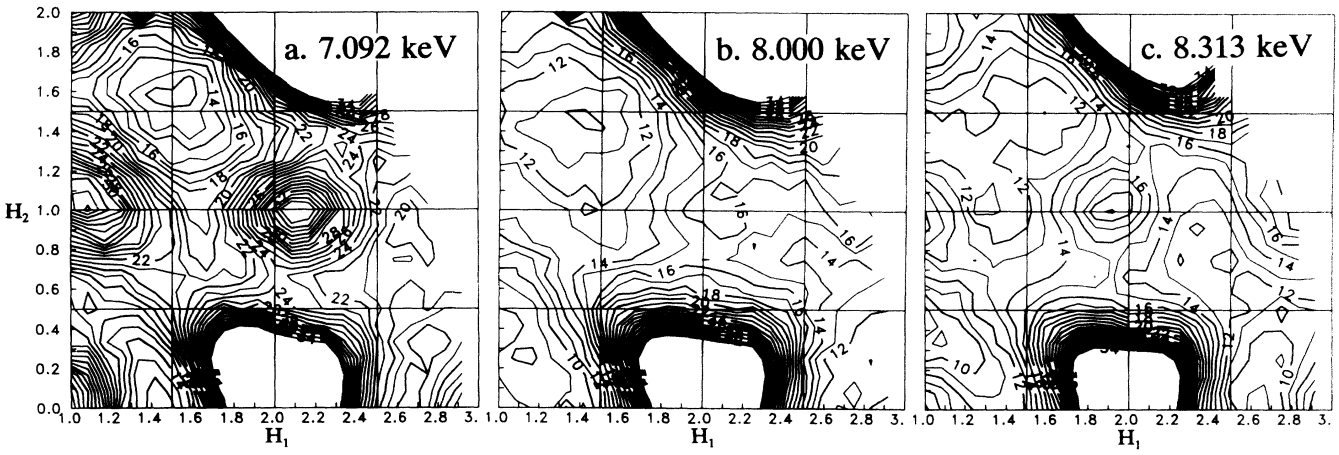

FIG. 1. Diffuse x-ray scattering intensities in the $H_3=0$ plane collected with x-ray energies of (a) 7.092, (b) 8.000, and (c) 8.313 keV. TDS which peaks near the 200 and 220 Bragg positions is later removed by subtracting the 8-keV data where $f_{Ni}\simeq f_{Fe}$. The weaker SRO peaks near the superstructure positions 100, 110, 120, and 210 are changed in intensity and shifted by I_{SD} when the magnitude of $f_{Ni}-f_{Fe}$ is changed and the sign reversed.

tions about either the distribution of the thermal diffuse scattering (TDS) or its temperature dependence [11,13]. Here, we make neither of these assumptions.

The experiment was performed at the Oak Ridge National Laboratory beam line at the National Synchrotron Light Source [14]. Scattered x rays were dispersed by a graphite mosaic crystal spectrometer [15] to permit experimental removal of the inelastic Compton and resonant Raman scattering [16]. The sample was a polished $Fe_{22.5}Ni_{77.5}$ single crystal.

The measured elastic diffuse scattering maps of I_T in the $H_3=0$ plane in electron units for the three energies are shown in Fig. 1. (Note that $H=2h$ so that the Miller indices of the Bragg reflections have their usual values.) Data were taken in a volume for cubic symmetry and $H^2\leq 9$. Intense thermal diffuse scattering is observed near the 200 and 220 fundamental Bragg reflections. Of interest are the small and diffuse SRO peaks near the

TABLE I. Short-range order coefficients α_{lmn} and the size-effect displacement components in Å for $Fe_{22.5}Ni_{77.5}$ quenched from 1000 °C compared with neutron data on $Fe_{23.5}Ni_{76.5}$ quenched from 520 °C and the fully ordered state of Ni_3Fe. The x displacement component (Δ_x) for each l,m,n is given as well as the magnitude of the displacement along the interatomic vector l,m,n (Inter.) for $Fe_{22.5}Ni_{77.5}$.

	α_{lmn}			Ni-Ni Pairs		Ni-Fe Pairs		Fe-Fe Pairs	
Shell l,m,n	X-Ray 22.5% Fe	Neutron 23.5% Fe	Theory Ni_3Fe Ordered	$\langle\Delta_x\rangle_{lmn}$ (Å)	Inter. (Å)	$\langle\Delta_x\rangle_{lmn}$ (Å)	Inter. (Å)	$\langle\Delta_x\rangle_{lmn}$ (Å)	Inter. (Å)
000	0.990(13)	0.946	1.000	0	0	0	0	0	0
110	-0.155(7)	-0.110	-0.333	-0.00016(8)	-0.00022(12)	-0.0015(3)	-0.0022(4)	0.030(2)	0.043(3)
200	0.128(8)	0.138	1.000	0.00002(22)	0.00002(22)	0.0026(10)	0.0026(10)	-0.011(2)	-0.011(2)
211	-0.016(5)	-0.010	-0.333	0.00035(7)	0.00023(6)	-0.0005(2)	-0.0001(2)	-0.001(1)	-0.002(1)
112	-0.016(5)	-0.010	-0.333	-0.00008(5)	0.00023(6)	0.0004(2)	-0.0001(2)	-0.002(1)	-0.002(1)
220	0.021(7)	0.055	1.000	-0.00065(13)	-0.00091(18)	0.0000(5)	0.0001(7)	0.007(2)	0.010(2)
310	-0.022(4)	-0.025	-0.333	0.00048(8)	0.00046(8)	-0.0015(3)	-0.0014(3)	0.006(1)	0.005(1)
103	-0.022(4)	-0.025	-0.333	0.00003(8)	0.00046(8)	0.0002(3)	-0.0014(3)	-0.002(1)	0.005(1)
222	0.016(5)	0.033	1.000	-0.00029(9)	-0.00049(16)	0.0010(3)	0.0017(6)	-0.003(1)	-0.006(2)
321	-0.012(3)	-0.011	-0.333	0.00011(4)	0.00017(4)	-0.0004(2)	-0.0006(2)	0.002(1)	0.002(1)
213	-0.012(3)	-0.011	-0.333	0.00016(4)	0.00017(4)	-0.0003(2)	-0.0006(2)	-0.000(1)	0.002(1)
132	-0.012(3)	-0.011	-0.333	0.00000(5)	0.00017(4)	-0.0003(2)	-0.0006(2)	0.002(1)	0.002(1)

100, 110, 120, and 210 superstructure positions. At 7.092 keV $f_{Ni}-f_{Fe}$ is positive, and as a result the displacements of the SRO peaks from the superlattice positions of Fig. 1(a) are opposite to that observed in Fig. 1(c) at 8.313 keV, where $f_{Ni}-f_{Fe}$ is negative. This change in position, shown here for the first time, arises from the sign change in $f_{Ni}-f_{Fe}$, Eqs. (1c) and (1d), and provides a vivid illustration of the aperiodic positioning of the SRO peaks caused by static displacements of the atoms. At 8.000 keV the x-ray scattering contrast between Fe and Ni is small (primarily imaginary), and the short-range-order peaks are weak, Fig. 1(b). These data were used to remove the TDS from the data taken at 7.092 and 8.313 keV by an iterative technique [17].

The measured SRO coefficients, α's, are given in Table I along with those measured with neutrons in a $Fe_{23.5}Ni_{76.5}$ crystal [18]. Table I also contains both the components of the displacements and the displacements resolved along the interatomic vector between atom pairs for ease of comparison with the hard-sphere model. Both the α's and the displacements are recovered by a linear least-squares fit to the data expressed as the sum of Eqs. (1a) and (1b). The uncertainties given in the table are determined by propagating the estimated errors in the normalization constants and the statistical errors in the collected data. The coefficients α_{000}, which should equal 1, and Δ_{110} are particularly sensitive to the relative normalization of the three data sets. Simulations of $I(h)_{SRO}+I(h)_{SD}$ from these recovered coefficients, labeled FIT in Fig. 2, closely reproduce the measured intensity, labeled DATA. The previous neutron measurement of $Fe_{23.5}Ni_{76.5}$ quenched from $-535\,^{\circ}C$ showed no obvious displacements of the SRO maxima from the superlattice. Atomic displacement coefficients about 10 times smaller than the values reported here were recovered by assuming close packing of spheres [18]. Their SRO coefficients are similar to the x-ray values.

We observe that the Ni-Ni atom pairs have small displacements from the average lattice while Fe-Fe atom pairs undergo much larger displacements: 0.043(4) Å between [110] first-neighbor pairs. As there are no established theories with which to predict the Fe-Fe, Ni-Ni, and Ni-Fe separations, we compare our direct measurements to the hard-sphere model, which assumes atoms are in contact along their close-packed direction. Pure Ni has a face-centered-cubic (fcc) room-temperature lattice parameter which corresponds to a hard-sphere diameter of 2.491(2) Å [19], and pure fcc Fe has a hard-sphere diameter of 2.527(4) Å [20], corrected for thermal expansion to 300 K. The predicted [110] distance for $Fe_{22.5}Ni_{77.5}$ with pure-element hard spheres is 2.499(4) Å which is less than the measured average [110] distance of 2.512(3) Å. We find that both Ni-Ni and Fe-Fe [110] distances correspond to diameters larger by -0.02 to 0.03 Å than predicted from pure-element hard spheres. However, the measured Ni-Fe [110] distance is close to the pure-element hard-sphere prediction and -0.02 Å shorter than the average of the Ni-Ni and Fe-Fe [110] distances in the alloy. Thus the direct measurements cannot be explained by a hard-sphere model.

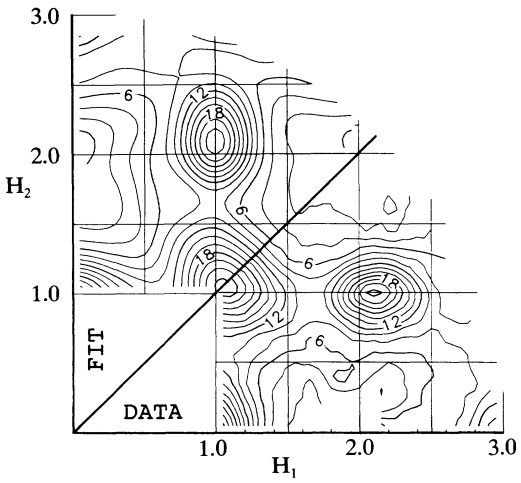

FIG. 2. The diffuse intensity distribution (FIT) calculated from recovered α's and pair displacement terms are compared with the measured intensity (DATA) at 7.092 keV in the $H_3=0$ plane. The intensities are well matched across the 45° symmetry axis.

Within the local spin-density (LSD) theory, the magnetic state of fcc iron and iron in iron-containing fcc alloys is very sensitive to atomic volume [21]. In LSD calculations at [110] spacings larger than 2.55 Å, fcc iron is predicted to be in a high spin ferromagnetic state. Below this a low spin state is stable, which may be antiferromagnetic or nonmagnetic. At the average [110] spacing of 2.51 Å for $Fe_{22.5}Ni_{77.5}$, hypothetical fcc Fe would be in the low spin state. However, fcc iron with a [110] spacing of 2.554(3) Å, consistent with our measured Fe-Fe separation, would be in the high spin state. Neutron-diffraction measurements on disordered Ni_3Fe place Fe in the high spin state with a magnetic moment of $3.13\mu_B$ [22].

A feature of the calculated electronic structure of disordered Fe-Ni alloys [23] is that, in the ferromagnetic state, the iron and nickel majority d electrons form a common band. This results from the large exchange splitting on the iron sites and leads to a reduction of the electronic kinetic energy compared to the nonmagnetic state. A reduced Fe moment in a Fe-Ni alloy would result in a smaller exchange splitting, split-band behavior of the majority electrons, and an increase in kinetic energy. We propose that the measured Fe-Fe dilation may be driven by a reduction in electron kinetic energy resulting from the Fe sites being in a large volume, high spin, state.

We have shown that meaningful individual pair displacements can be recovered with sufficient accuracy to provide tests of magnetic and solid solution size-effect

theories and to challenge theorists to include static displacements in their *ab initio* calculations of phase stability. With our method of removing TDS, measurements at temperature, to ensure equilibrium structures, are more plausible. The method described here has also been applied to a clustering solid solution of $Fe_{53}Cr_{47}$ [24]. Measurements of atomic displacements and SRO are underway for a series of Ni-Fe alloys through the Invar composition.

We appreciate comments by G. M. Stocks. This work was sponsored by the Division of Materials Sciences and Division of Chemical Sciences, U.S. Department of Energy, under Contract No. DE-AC05-84OR21400 with Martin Marietta Energy Systems, Inc., and under contract with the National Synchrotron Light Source, Brookhaven National Laboratory.

[1] J. M. Cowley, J. Appl. Phys. **21**, 24 (1950).

[2] V. Gerold and J. Kern, Acta Metall. **35**, 393 (1987).

[3] K. Binder, J. L. Lebowitz, M. K. Phani, and M. H. Kaos, Acta Metall. **29**, 1655 (1971).

[4] F. J. Pinski, B. Ginatempo, D. D. Johnson, J. B. Staunton, G. M. Stocks, and B. L. Gyorffy, Phys. Rev. Lett. **66**, 766 (1991).

[5] See, for example, *Electronic Structure, Dynamics, and Quantum Structural Properties of Condensed Matter*, edited by J. T. Deveneese and P. Van Camp, NATO Advanced Study Institutes, Ser. B, Vol. 121 (Plenum, New York, 1984); A. Zunger, S.-H. Wei, L. G. Ferreira, and J. E. Bernard, Phys. Rev. Lett. **65**, 353 (1990); J. S. Louvel, in *Magnetism and Metallurgy*, edited by A. E. Berkowitz and E. Kneller (Academic, New York, 1969), Vol. 2; E. F. Wassermann, Adv. Solid State Phys. **27**, 85 (1987); F. Laves, *Theory of Alloy Phases* (American Society for Metals, Cleveland, OH, 1956), p. 124.

[6] T. G. Ramesh and S. Rameseshan, Acta Crystallogr., Sec. A **27**, 569 (1971).

[7] D. Sayers, in *X Ray Absorption: Principles, Applications, Techniques of EXAFS, SEXAFS, and XANES*, edited by R. Priazand and D. C. Keningsberger (Wiley, New York, 1987).

[8] J. E. Tibballs, J. Appl. Cryst. **8**, 11 (1975); P. Georgopoulos and J. B. Cohen, Acta Metall. **29**, 1535 (1981); X. Auvray, P. Georgopoulos, and J. B. Cohen, Acta Metall. **29**, 1061 (1981).

[9] B. Borie and C. J. Sparks, Jr., Acta Crystallogr., Sec. A **27**, 198 (1971).

[10] C. B. Walker and D. T. Keating, Acta Crystallogr. **14**, 1170 (1961).

[11] B. E. Waren, *X-Ray Diffraction* (Dover, New York, 1969); B. E. Warren, B. L. Averbach, and B. W. Roberts, J. Appl. Phys. **22**, 1493 (1951); C. J. Sparks and B. Borie, *Local Atomic Arrangements Studied by X-Ray Diffraction* (Gordon and Breach, New York, 1966), pp. 1–46; J. E. Gragg and J. B. Cohen, Acta Metall. **19**, 507 (1971).

[12] D. T. Cromer and D. Liberman, J. Chem. Phys. **53**, 1891 (1970).

[13] B. Borie and C. J. Sparks, Jr., Acta Crystallogr. **17**, 827 (1964).

[14] A. Habenschuss, G. E. Ice, C. J. Sparks, and R. Neiser, Nucl. Instrum. Methods Phys. Res., Sec. A **266**, 215 (1988).

[15] G. E. Ice and C. J. Sparks, Nucl. Instrum. Methods Phys. Res., Sec. A **291**, 110 (1990).

[16] C. J. Sparks, Phys. Rev. Lett. **33**, 262 (1974).

[17] G. E. Ice, C. J. Sparks, and L. B. Shaffer (to be published).

[18] S. Lefebvre, F. Bley, M. Fayard, and M. Roth, Acta Metall. **29**, 749 (1981).

[19] *Pearson's Handbook of Crystallographic Data for Intermetallic Phases*, edited by Y. P. Villars and L. D. Calvert (American Society for Metals, Metals Park, OH, 1985).

[20] E. A. Owen and A. H. Sully, Philos. Mag. **31**, 314 (1941).

[21] F. J. Pinski, J. Staunton, B. L. Gyorffy, D. D. Johnson, and G. M. Stocks, Phys. Rev. Lett. **56**, 2096 (1986).

[22] J. W. Cable and E. O. Wollan, Phys. Rev. B **7**, 2005 (1973).

[23] D. D. Johnson, F. J. Pinski, and G. M. Stocks, J. Appl. Phys. **57**, 3018 (1985).

[24] L. Reinhard, J. L. Robertson, S. C. Moss, G. E. Ice, P. Zschack, and C. J. Sparks, Phys. Rev. B (to be published).